Experimental and Computational Investigation of Isothermal Swirling Flow in an Axisymmetric Dump Combustor

S. C. Favaloro*
Aeronautical Research Laboratory, Melbourne, Australia
and
A. S. Nejad† and S. A. Ahmed†
Aero-Propulsion and Power Laboratory,
Wright Patterson Air Force Base, Ohio 45433

Experimental and theoretical studies of nonreacting swirling flow have been performed in a model of an axisymmetric dump combustor. A two-component laser Doppler velocimeter was used to obtain measurements of the three velocity components and numerous fundamental turbulence quantities in two series of tests with minimum disturbance to the combustor flowfield. The results showed the significant effects of swirl, with and without vortex breakdown, on the mean and turbulent flowfields. The experimental results were used to check the performance of a recently developed computer program which used the k-ε closure model. Comparisons of the numerical and experimental results showed the inadequacy of the k-ε turbulence model in representing the complex structure of confined swirling flows.

Nomenclature

H	= step height, 0.5 R_{in}
k	= turbulent kinetic energy, $(u'2 + v'^2 + w'^2)/2$
S	= swirl number
U,V,W	= time mean axial, radial, and tangential velocities
u',v',w'	= axial, radial, and tangential rms turbulent velocities
X,R	= axial and radial coordinates
ε	= dissipation rate, $k^{1.5}/0.3\ R_{in}$

Subscripts

h	= swirler hub
in	= inlet conditions
ref	= inlet centerline value

Introduction

THE development of gas turbine and ramjet propulsion systems can be facilitated utilizing advanced design codes. Complementary experimental and theoretical studies of the combustor flowfield are essential to check the validity of these codes. Flowfields in combustors of current practical interest involve regions of highly turbulent recirculating flow. The number and size of these regions vary according to the combustor geometry and/or the strength and type of swirl imparted to the incoming flow. Such regions promote rapid fuel/air mixing and enhance flame stabilization, which lead to improved combustion efficiency, better blowoff limits, and a reduction in the formation of particulates and gaseous pollutants.

Extensive studies of the effect of swirl in a variety of combustor geometries have been reported in the literature. Different concepts such as a single confined jet expanding into a larger tube (dump combustor),[1-6] freejets,[7,8] coaxial confined jets,[9-13] and multijet tangential entries[14] have been investigated. Buckley et al.[1] have shown the considerable impact of different swirl profiles on the efficiency and pressure recovery of dump combustors, while Kilik[15] has demonstrated the effects of swirl vane angle curvature on the size of the induced recirculation zone. Different methods of swirl generation and characterization have been discussed at some length by Beer and Chigier[16] and Gupta et al.[17] For the interested reader, a thorough review of swirling flows has been compiled by Lilley.[18]

Because of the complexity of these types of flows, combustor design methodology has been based on accumulated engineering design experience combined with empirical correlations from extensive trial and error development tests. Currently, much of the research effort has been aimed at reducing this uneconomical and somewhat inefficient approach to combustor design. The application of numerical methods can be of immense benefit to the design procedure, provided the flowfield can be predicted. Unfortunately, progress in the realistic solution of swirling, reacting, and highly turbulent recirculating flows has been limited due to the inherent complexity of such flows and, to a larger extent, to the lack of detailed experimental data that are required to calibrate and check the validity of any numerical model used and to justify the assumptions that are made to ensure closure in the time-mean solution of the Navier-Stokes equations.

Laser-based optical techniques appear to be one of the most suitable experimental methods for obtaining detailed and accurate data in highly complex flowfields. Unlike more conventional techniques, such as the hot-wire anemometer and pitot probes, optical methods do not cause flow disturbance or suffer from directional ambiguity and are generally able to cope with high levels of turbulent fluctuations. Because of their nonintrusive nature, they are the only practical method of making measurements in flames. The major drawbacks with LDV techniques are the requirements to adequately seed the measurement region with particles that follow the flow and to ensure access through test section walls that is predominantly free of optical aberration.

Before attempting to understand the role of combustion processes in determining the combustor flowfield, there is obvious benefit in considering the isothermal case. With this step-by-step approach, useful information on nonreacting fluid mechanical phenomena, such as mass and momentum exchange, kinetic energy dissipation, etc., can be obtained without the complicating effects of chemical reaction and heat

Received Jan. 4, 1989; presented as Paper 89-0620 at the AIAA 27th Aerospace Sciences Conference, Reno, NV, Jan. 9-12, 1989; revision received Oct. 2, 1989; accepted for publication Dec. 15, 1989.

*Mechanical Engineer.
†Aerospace Engineer.

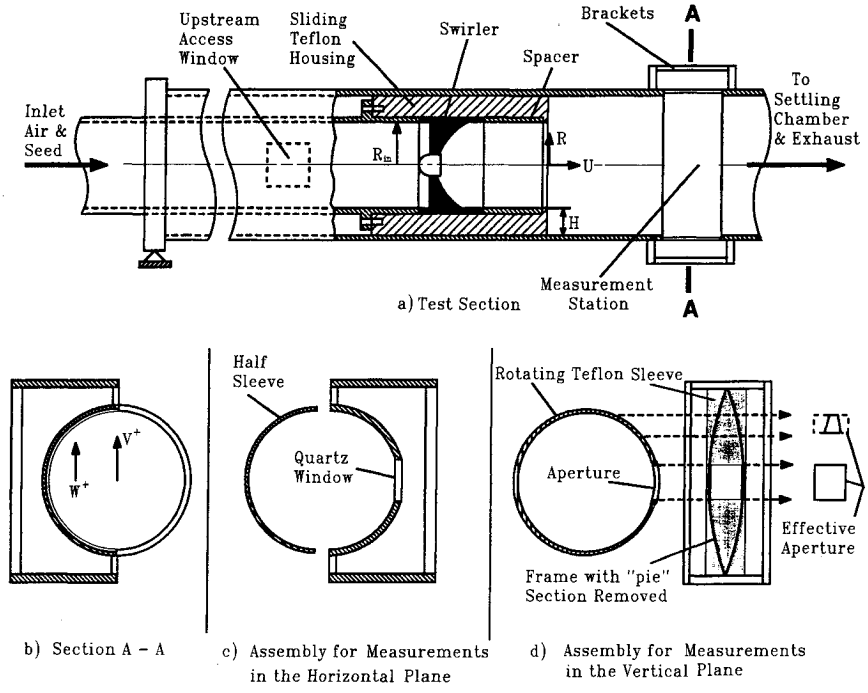

Fig. 1 Schematic of model combustor.

release. The present study focuses on the effects of swirl on the flowfield in an isothermal dump combustor. It is a part of an ongoing program[1-3] aimed at providing benchmark quality data to assist in the understanding of swirling flows and to aid in the improvement of a recently developed computer program that utilizes the k-ε closure model.

The current study complements the work of Ref. 2 and provides the radial component of the velocity field which was not reported earlier. Since turbulence in swirling flows is not isotropic, the inclusion of the radial fluctuating component of the velocity field is imperative for the calculation of turbulent kinetic energy k. To accomplish this task, measurements were made along the vertical diameter, whereas the results of Ref. 2 were obtained from measurements along the horizontal diameter.

In this manuscript, a near complete set of velocity and turbulence data is presented. The tangential component of the velocity field is borrowed from the reported results of Ref. 2. The present data cover sub- and supercritical swirl number, i.e., with and without a central recirculation zone. To the best of the authors' knowledge, such detailed and complete experimental observations of the velocity field for this particular geometry have not been published in the open literature.

Experimental Facility

Combustor Geometry

The present experiments were conducted in the axisymmetric dump combustor model shown schematically in Fig. 1a. The working fluid was air, which was pushed through the model by a centrifugal-type blower. The most important design criterion was the simultaneous requirement of preserving the integrity of the axisymmetric flowfield and providing excellent optical access for two-component laser velocimetry. To satisfy this criterion, a modular research combustor, which consisted of two major sections, namely an inlet assembly and a combustion chamber, was designed and fabricated.

Inlet Assembly

The inlet assembly consisted of a 300-mm-diam settling chamber, a Plexiglas inlet pipe (2850 mm in length and 101.6 mm i.d.), and a cylindrical Teflon swirler housing (104.5 mm i.d., 152.4 mm o.d., and 154 mm in length). The swirler and a spacer, which enabled the swirler to be located either at the dump plane or 50.8 mm upstream, were incorporated in the housing. Throughout this study and those of Refs. 1 and 2, the swirlers were placed 50.8 mm upstream of the dump plane. In order to examine the characteristics of the flow upstream of the swirler with LDV, a flat 38 × 38 mm optical quality quartz window was installed in the inlet pipe 50.8 mm upstream of the swirler housing (see Fig. 1a). The window was replaced by a plug with the same radius of curvature as the inlet pipe when measurements in the combustor were performed, thereby eliminating any inlet flow disturbances. A unique feature of the design was the capability of positioning the dump plane (swirler housing) relative to the measurement location in the combustion chamber. This was accomplished by supporting the entire inlet assembly on a traversing mechanism controlled by a stepping motor. Throughout the experiments, the inlet centerline velocity was monitored with a pitot tube located 1400 mm upstream of the swirler housing and was maintained at 19.2 ± 0.4 m/s, corresponding to a Reynolds number of 1.25×10^5 based on combustor inlet diameter.

Swirlers

Two constant angle axial flow-type swirlers, designed by Buckley et al.,[1] with swirl numbers of 0.3 and 0.5 were used in this study. Swirl number S is defined as

$$S = \int_{R_h}^{R_{in}} U\,WR^2 dR \,/\, (R_{in} \int_{R_h}^{R_{in}} U^2\,R\,dR) \qquad (1)$$

Each swirler had 12 circular arc inlet guide vanes welded between a 101.6-mm outer ring and a 19-mm central hub. The leading edge of each blade was designed to be tangent to the incoming flow and perpendicular to the centerline of the combustor model.

Combustion Chamber

This section consisted of a Plexiglas tube (152.4 mm i.d. and 1850 mm in length) terminating in a large rectangular settling chamber (1210 × 890 × 890 mm) also fabricated from Plexiglas for flow visualization studies. At the designated measurement station, 865 mm from the combustor exit, a 14-mm-wide section (extending from the top to the bottom of the pipe) was removed to accommodate one of the two window assemblies

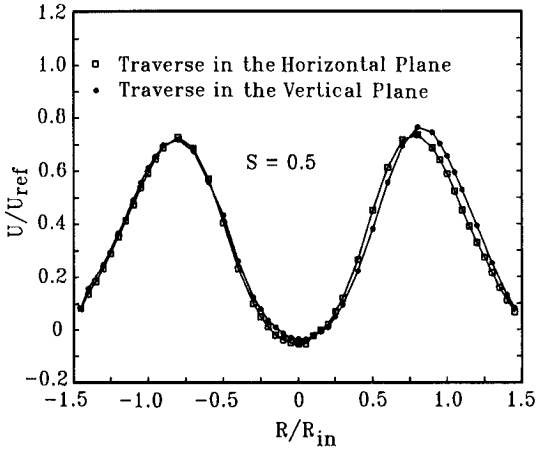

Fig. 2 Axial velocities in the horizontal and the vertical planes.

shown in Figs. 1a and 1b. A recess, 2 mm deep and 40 mm wide, was cut in the opposite section of the pipe. Earlier experiments,[2,3] were conducted with a 30-deg contraction nozzle at the combustor exit. The current data demonstrated that the effects of the nozzle on the flowfield at the measurement location were insignificant for the present setup. Similar results were also reported earlier by Lilley.[4]

Window Assemblies

Figure 1c shows the arrangement when velocity measurements were made in the horizontal plane. This assembly consisted of a flat 38 × 38 mm optical quality quartz window installed in a frame fabricated from 152.4-mm-i.d. Plexiglas. The frame was bonded to two brackets and attached to the combustor section as shown in Fig. 1. A 40-mm-wide half-sleeve, fabricated from 152.4-mm-i.d. Teflon, was located in the combustor wall recess to ensure a smooth flow passage. The whole assembly was sealed with vacuum grease to prevent leakage. Figure 1d shows the arrangement for performing velocity measurements in the vertical plane. This assembly consisted of a frame, fabricated from 154.4-mm-i.d. Plexiglas, with a pie-shaped section removed from it, and a rotating Teflon sleeve, 40 mm wide, 2 mm thick, and 152.4 mm i.d., with a 30 × 20 mm centrally located rectangular aperture. The assembly was mounted on the combustor section as described previously. The frame/sleeve combination provided the minimum optical access opening as the LDV was traversed in the vertical plane while simultaneously minimizing flow disturbance as shown in Fig. 1d. The results from typical LDV traverses in the horizontal and vertical planes are shown in Fig. 2. These results illustrate the symmetry of the combustor flowfield and show how the integrity of the flow has been preserved with both optical window assemblies.

Laser Velocimeter

The optical system used in these experiments was a two-component TSI Inc. four-beam two-color backscatter system with several in-house modifications as described in Ref. 2. The optics included two Bragg cells, a 3.75 beam expander with a 35-mm entrance beam separation and a final focusing lens of focal length 450 mm. The 488-nm (blue) and 514.5-nm (green) lines of an argon-ion laser operating at 300 mW were used in all measurements. The approximate measurement volume dimensions based on $1/e^2$ intensity points were 600 μm length and 80 μm diam. The system was configured so the fringe inclinations were 45.667 and 135.167 deg to the combustor centerline; to prevent fringe bias and to provide directional sensitivity, both sets of fringes were shifted at 40 MHz. The entire optical system was mounted on a three-axis traversing table, which allowed the probe volume to be positioned with a resolution of 0.025 mm.

A chemical seeder, first employed by Craig et al.,[19] which produced micron size TiO_2 particles was used in this study. To approach a uniformly seeded flow, the particles were introduced into the upstream throttling manifold of the centrifugal blower.

Data Acquisition and Analysis

The Doppler signals from the photomultipliers were processed by two TSI counter-type systems with low- and high-pass filters set at 100 MHz and 20 MHz, respectively, on each processor. Typical validated data rates, with comparator settings of 1% and fringe counts of 16 were between 5000 and 10,000/s. With the implementation of a 20-μs coincidence window, the subsequent coincidence data transfer rate ranged between 2000 and 5000/s. To reduce statistical uncertainties in the calculation of the higher-order moments of turbulent fluctuations, 27,300 samples per channel were collected at each measurement location. Data transfer to the dedicated ModComp/Classic II/75-5 computer system was accomplished in the DMA mode, at a maximum rate of 1 Mbyte/s through a custom-made interface. Double precision (48 bit) calculations of all statistical moments using standard formulas[20] were made at each measurement location. In most cases, the data were sufficiently noise-free to avoid the use of cutoff limits on the calculated velocity histograms.

The problem of velocity bias in LDV measurements has been examined thoroughly since first recognized by McLaughlin and Tiederman.[21] This error arises from the fact that counter-type signal processors make discrete velocity measurements from individual realizations of seed particles passing through the measurement volume. In a uniformly seeded flow, the number of particles per unit time passing through the measurement volume is proportional to the flow rate through that volume, and simple arithmetic averaging of an ensemble of realizations will produce results biased toward values greater than the true temporal mean. This effect is more pronounced in highly turbulent flows, and a number of different schemes have been proposed for its removal. The method adopted in the current study used the time between individual realizations (particle interarrival time) as a weighting factor.[2,19,20] The integrity of the system and the data acquisition software were checked in a simple freejet experiment, reported by Ahmed et al.[22] The uncertainty of the measured mean velocities was determined using the techniques described in Ref. 23. The uncertainty Δ is determined by the relation

$$\Delta U = \pm 1.96 S_u/N \tag{2}$$

For 95% confidence level, the constant 1.96 is used; S_u is an estimator for the true standard deviation, and N is the sample size. From the above relation, the maximum uncertainties of the mean quantities (i.e., U, V, W) due to random errors were found to be 0.4, 0.35, and 0.35% of the upstream centerline velocity, respectively.

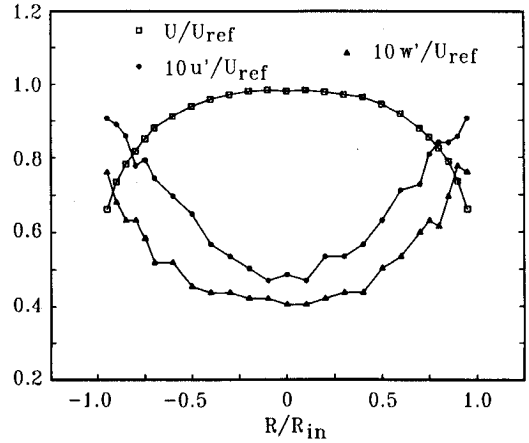

Fig. 3 Upstream flow conditions.

Numerical Approach

The experimental program described previously was complemented by an analytical effort which solved the Navier-Stokes equations in conjunction with a k-ε turbulence model. Since the equations which govern the flowfields of current interest are elliptic in space, their solution has usually entailed considerable computing time and cost, unless the number of nodes was reduced. A significant difference between the current approach and earlier ones is the use of a multigrid technique[24,25] and a coupled solution of the momentum and continuity equations, which enables accurate solutions to be obtained after 20 to 25 iterations independent of grid size.

The solution domain was taken to be 20 step heights long with zero derivative boundary conditions at the exit. The inlet boundary conditions were prescribed from measurements of the axial, radial, and tangential velocities at $X/H = 0.38$, while wall functions[26] were used to capture the effects of steep near-wall gradients. The solution was performed for one-half of the cross section only, with the assumption of symmetry about the centerline. The inlet turbulent kinetic energy and dissipation rates were calculated from

$$k = 0.5(u'^2 + v'^2 + w'^2) \tag{3}$$

$$\varepsilon = k^{1.5} / 0.3R_{in} \tag{4}$$

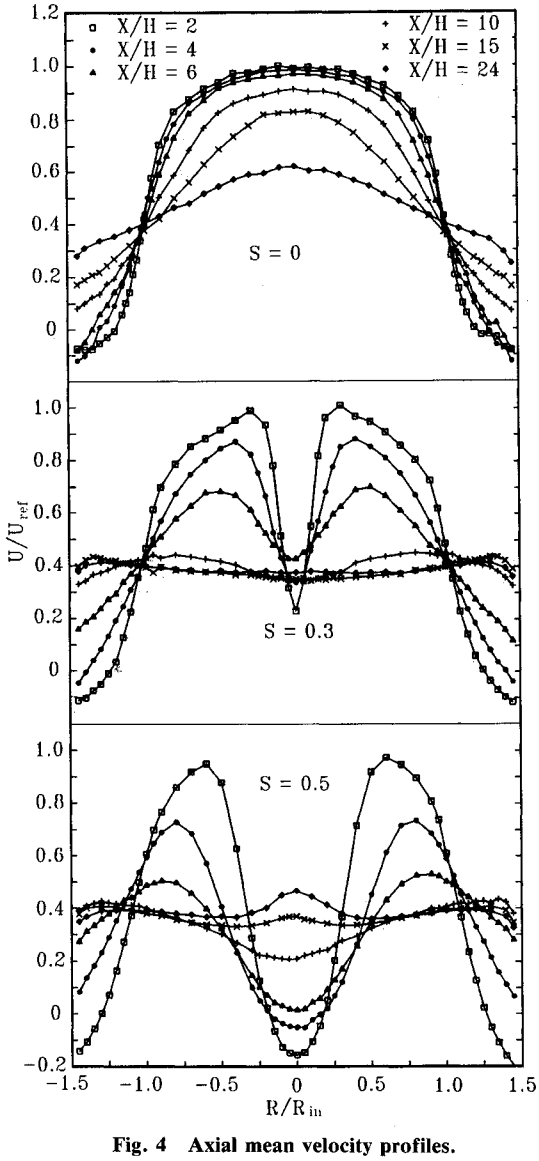

Fig. 4 Axial mean velocity profiles.

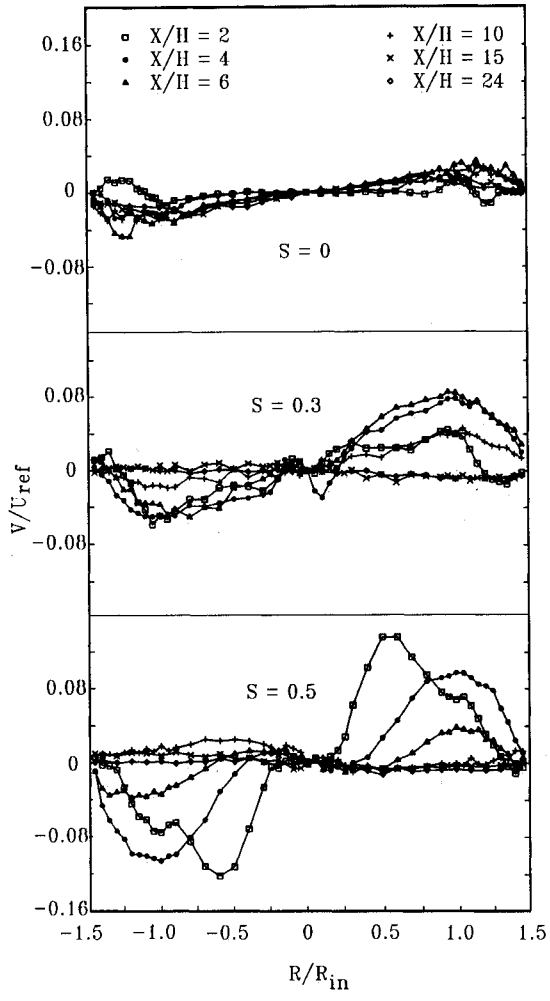

Fig. 5 Radial mean velocity profiles.

Since there are currently no means of measuring the dissipation rate [Eq. (4)], it was assumed to be constant over the entire inlet cross section. The calculations were performed for finite-difference grids consisting of 80 × 48 finite-difference cells in the axial and radial directions, respectively. In a previous study,[25] it was observed that results from an 80 × 48 grid and a coarser 40 × 24 grid agreed very closely. Further grid refinement beyond the 80 × 48 grid was not made because the near-wall y^+ value would then become less than the applicable range for the wall functions. However, in several other studies reported in Ref. 25, the procedure was applied to finer grids without any difficulty. The solution was terminated when the sum of residuals in the axial momentum equation was less than 0.5% of the inlet momentum. At this level, the maximum successive changes in the U, V, and W velocities were within 0.1% of typical inlet values.

Experimental Results and Discussion

Inlet Flow

The results from LDV measurements taken in the inlet pipe, 94 mm upstream of the swirler, are presented in Fig. 3. The profiles are typical of a fully developed pipe flow, with 4% tangential and 5% axial turbulent intensities at the center, increasing to 7 and 9% near the wall, respectively. Although the axial and tangential turbulent velocities were unequal, the anisotropic ratio was almost constant throughout the inlet pipe, varying between 1.3 and 1.4. The mean axial velocity profile is very smooth, illustrating the symmetry of the flow upstream of the swirler. No attempts were made to make measurements in the vertical plane to check the characteristics of the radial component.

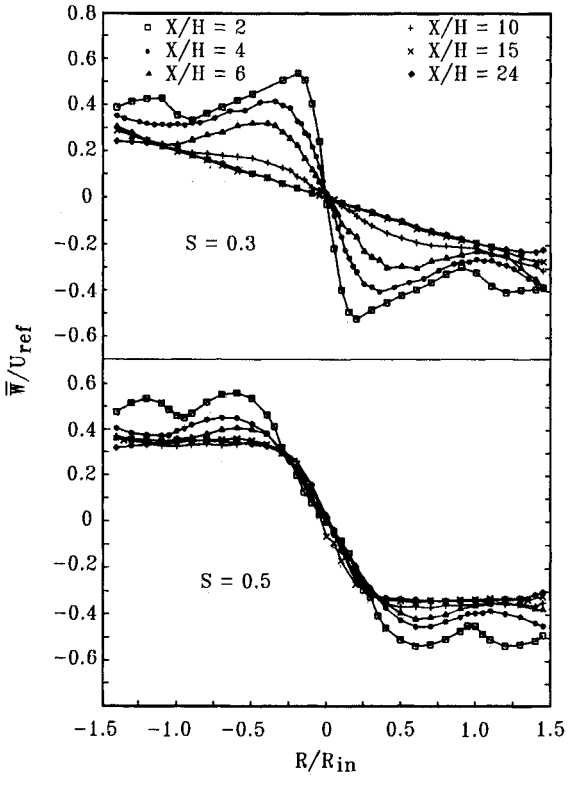

Fig. 6 Tangential mean velocity profiles.

Mean Flow

Figures 4–6 show the axial, radial, and tangential time-mean velocity profiles normalized with respect to the inlet centerline velocity, at selected streamwise locations for the three swirl levels. Measurements were made at seven other locations but have been omitted from the figures for clarity. With the exception of the tangential mean and fluctuating results, which have been reproduced from earlier measurements in the horizontal plane,[2] current data were performed in the vertical plane. A comparison of the axial mean and fluctuating velocity profiles presented in the current study with those of Ref. 2 substantiates the axisymmetric nature of the flowfield in the combustor model.

The significant impact of swirl on the axial mean flowfield is evident in Fig. 4. The major effects were in the core flow and the corner recirculation region. Vortex breakdown[27,28] occurred with the stronger swirling flow, establishing a central recirculating flow which extended to approximately 4.4 step heights downstream of the dump plane. The maximum diameter of this recirculating region was about one swirler hub diameter and was located roughly 3 step heights from the dump. The weaker swirling flow experienced a deceleration at the core of its central vortex, but it was insufficient to cause vortex breakdown. In addition, the axial velocity gradient at the centerline was much higher for the stronger swirling flow than the weaker case. The reduction in the length of the corner recirculation region, from approximately 8 step heights for the nonswirling flow to 4.3 and 3.2 step heights for the $S = 0.3$ and $S = 0.5$ flows, respectively, was caused by the rapid expansion of the flow after separation due to centrifugal forces. These aspects of swirling flows have also been reported by Lilley.[4]

The radial time-mean velocity profiles are shown in Fig. 5. For the flow with no swirl, the results exhibit characteristics of confined jets. For example, the radial flow direction in the core flow was toward the combustor walls. Near the dump plane, the radial flow changed direction, which correctly depicted the flow pattern in the corner recirculation region. This latter feature was not as evident in the swirling flow cases due to the reduction in the length of the corner recirculation region. However, it is clear that up to $X/H = 10$, the overall outflow is much stronger in the swirling flow cases with the maximum values in the $S = 0.5$ flow. A further significant feature of the $S = 0.5$ flow is the change in the general direction of the radial mean flow (toward the center) after $X/H = 10$ due to the strong expansion of the confined swirling jet. This accounts for the rapid redevelopment of the mean axial centerline flow shown in Fig. 4.

The tangential mean velocity field behavior is illustrated in Fig. 6 (for $S = 0$, W was almost zero). Although both flows initially showed profiles typical of dump combustor flow[4] and similarities to lifting surface leading-edge or trailing-edge vortex flows,[29] they exhibited totally different behavior farther downstream. For example, the weaker swirling flow expanded its vortex core at the expense of losing its strength and became a forced vortex downstream of $X/H \geq 10$ while the stronger swirling flow maintained the strength of its core up to the last measurement station, $X/H = 24$.

Turbulent Velocities

Figure 7 shows the axial rms turbulent velocities for the three swirl levels. This data matches the previous data set[2] where measurements were performed in the horizontal plane. As discussed in Ref. 2, the flow with no swirl revealed local peak values in the shear layer generated between the core flow

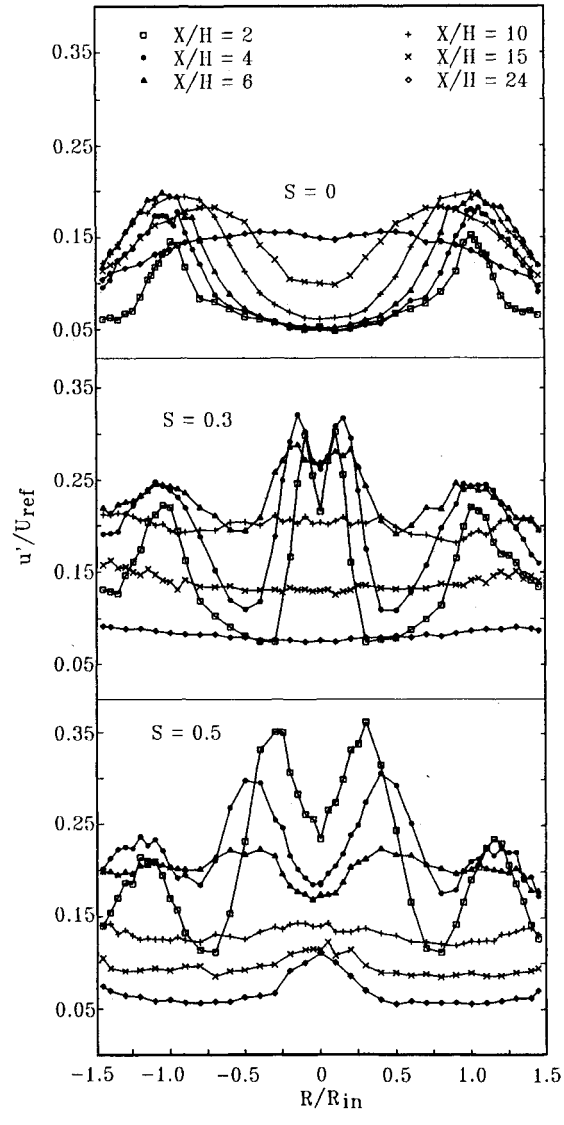

Fig. 7 Axial turbulent velocity profiles.

and the corner recirculation region, while an additional peak at the edge of the central vortex core was evident in both swirling flows. The decay of the turbulent velocities in the streamwise direction was much faster in the swirling flows than in the no swirl case, indicating that diffusion and dissipation rates are increased markedly by swirl. The previous work[2] also alluded to the fact that in the $S = 0.3$ flow, the axial turbulent velocities within the shear layer generated by the corner recirculation were higher than the ones generated by the stronger swirling flow at the same location. This feature was apparent in the current results although it was not as pronounced.

The radial and tangential turbulent velocity profiles are shown in Figs. 8 and 9, respectively. For the flow with no swirl, both sets of profiles were similar to the axial profiles. The anisotropic ratios varied between 1.6 and 1.1 throughout the flowfield, with peaks (maxima) in u'/v' occurring in the wall boundary layer and the shear layer at the edge of the recirculation region, while local maxima in u'/w' occurred halfway between the shear layer and the centerline flow. For $S = 0.3$ flow, local maximum values of both radial and tangential fluctuating velocities were found in the core of the central vortex and in the shear layer at the edge of the corner recirculation. These decayed rapidly as the flow reattached and as the vortex expanded to cover the entire combustor. The stronger swirling flow showed similar behavior in the aforementioned shear layer but was significantly different in

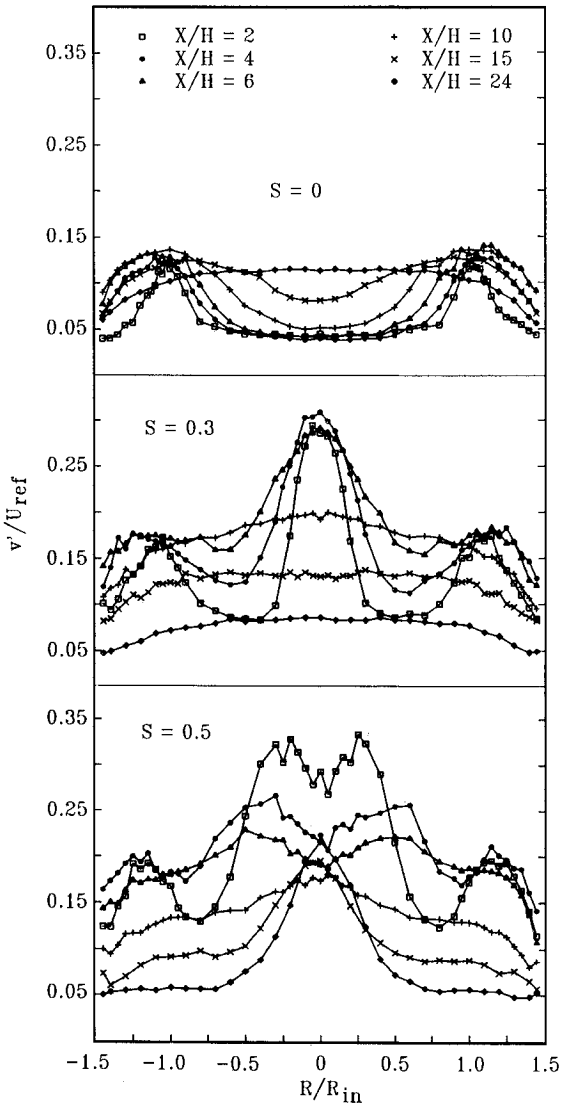

Fig. 8 Radial turbulent velocity profiles.

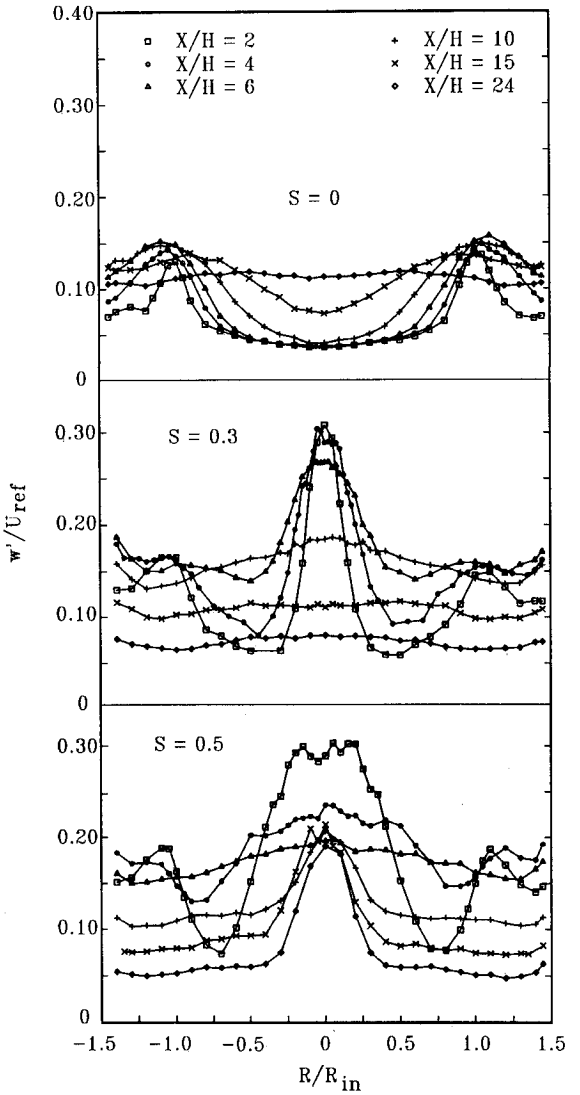

Fig. 9 Tangential turbulent velocity profiles.

the core flow. Up to $X/H = 6$, the maximum values were not clearly defined and appeared to be spread over the entire central recirculation region. After 6 step heights, peak values were found in the core of the vortex only and were maintained until the last measurement station. This is consistent with the mean flowfield behavior (Figs. 4–6), as high values of radial turbulent velocity are expected to contribute to the development of the tangential velocity field farther downstream of the last measurement station. The anisotropic ratio varied significantly throughout the combustor flowfield for the swirling flows. Both u'/v' and u'/w' dropped below 0.5 in the vortex core just downstream of the central recirculation region for $S = 0.5$ flow, while the minimum values for $S = 0.3$ occurred at the first measurement station downstream of the dump plane.

Shear Stresses and Triple Products

Profiles of the Reynolds shear stress in the vertical and horizontal planes ($\overline{uv}$ and $\overline{uw}$) are shown in Figs. 10 and 11. The third component $\overline{vw}$ cannot be obtained in the current combustor model with the two-component LDV system. For both swirling flows, local peaks in the vertical plane (Fig. 10) occurred at the edge of the vortex core and in the shear layer between the core flow and the corner recirculation region, while peaks for the flow with no swirl were obtained in the corner shear layer only. Prior to reattachment, Reynolds stress components in the vertical plane were higher in the stronger swirling flow, even though the gradients in the vortex core were

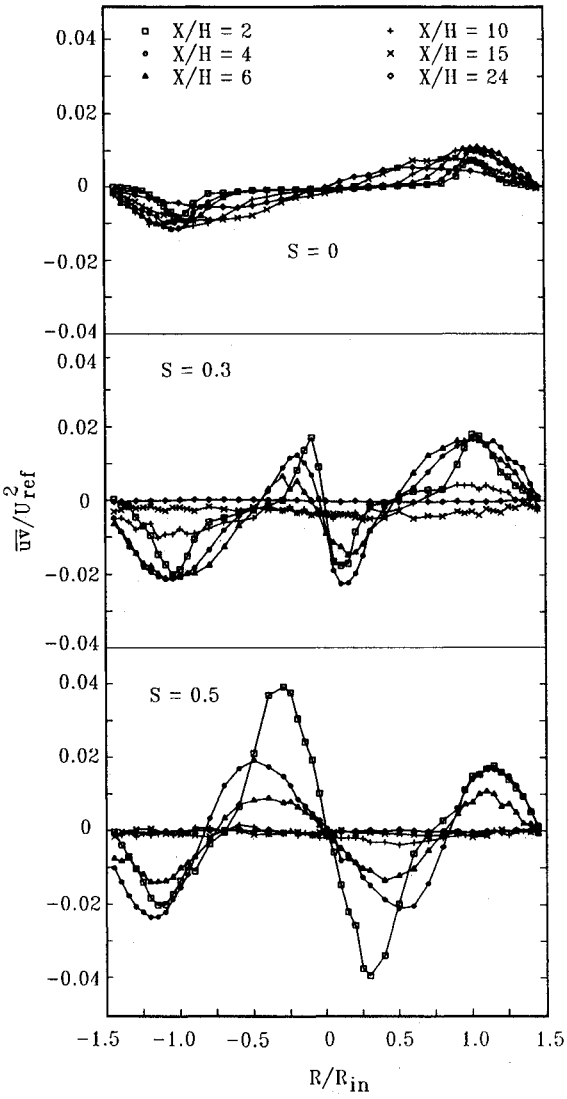

Fig. 10 Shear stress in the vertical plane.

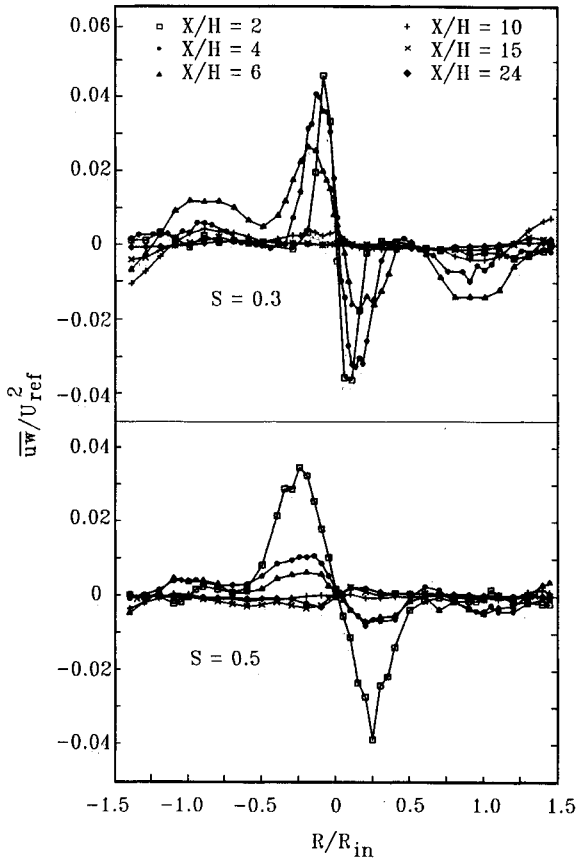

Fig. 11 Shear stress in the horizontal plane.

steeper in the weaker swirl case. High Reynolds stresses at the edge of the vortex core are a reflection of strong shear forces between the outer flow and the vortex core. The shear stress in the horizontal plane (Fig. 11) showed similar behavior, except that the maximum values occurred in the weaker swirling flow. These higher values can be attributed to two factors, as discussed in Ref. 2. First, the weaker swirling flow maintained a stronger vortex core up to 4 step heights downstream of the dump plane as shown by the larger tangential velocity gradients (see Fig. 6); second, flow instabilities, in the form of large-scale oscillations of the central vortex core, were more pronounced in the weaker swirling flow as discussed in Ref. 3. The interested reader should consult Ref. 3 in which flow instabilities were discussed in detail and their frequencies and power contents were reported.

A common feature of both shear stress components is that the rate of decay of the peak values in all shear layers is strongly dependent on the swirl strength, with the maximum rate occurring in the stronger swirling flow. Values of shear stress in the horizontal plane for the flow with no swirl were up to 20 times less than those in the swirl flows and are not shown.

Figure 12 shows profiles of triple products of turbulent velocities for both swirling flows. This product can be interpreted as the axial convection of turbulent kinetic energy. Large values of this transport term infer the presence of organized structures in the flowfields. Maximum values of axial convection occurred around the edges of the vortex cores for

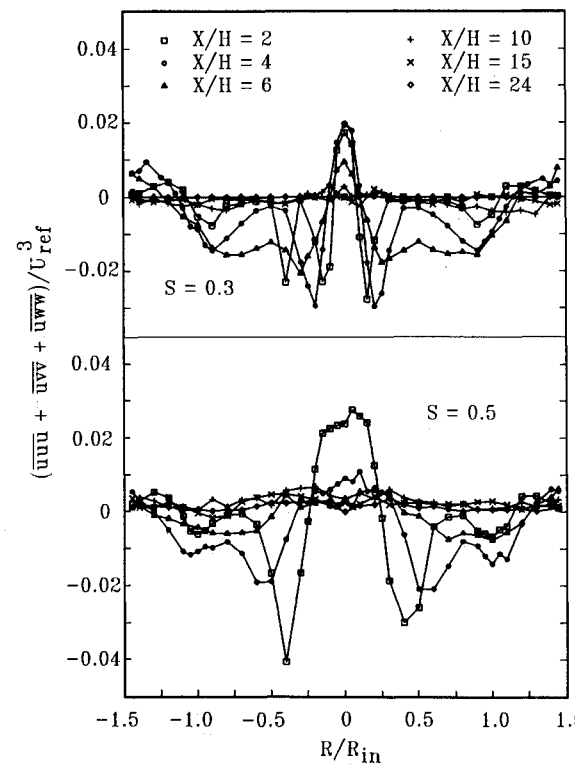

Fig. 12 Axial convection of turbulent kinetic energy.

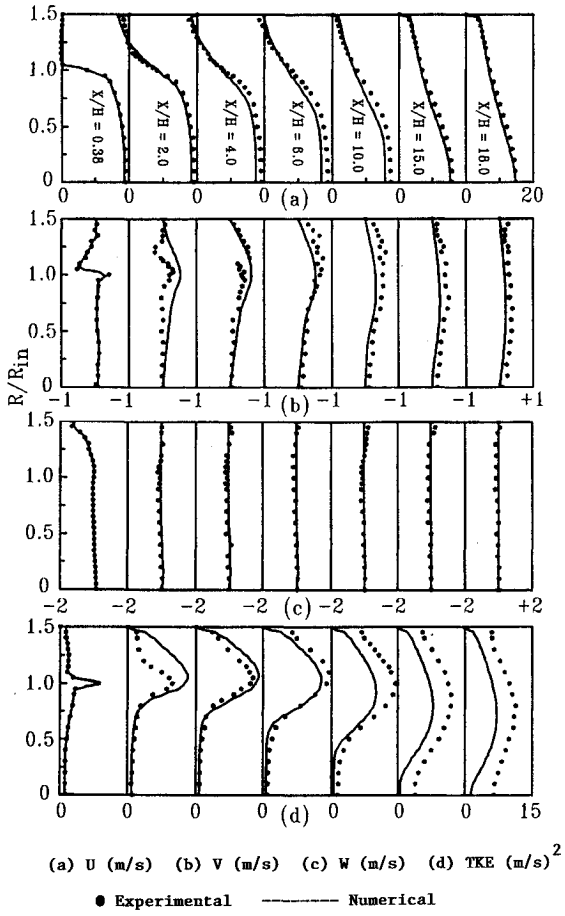

Fig. 13 Numerical/experimental comparisons for $S = 0$.

both flows and were consistent with the fast development of the mean flowfield at the core boundaries.

Comparison with Numerical Results

Figures 13–15 show comparisons of measured and calculated mean velocity components and turbulent kinetic energy for the three swirl levels investigated. Measured axial, radial, and tangential mean and fluctuating velocities at $X/H = 0.38$ were taken as the initial conditions for the computations. Comparisons of the experimental results and the analytical predictions for the case of $S = 0$ (simple axisymmetric sudden expansion, Fig. 13) show that there was reasonable agreement in the mean velocity field, but large discrepancies were observed in the fluctuating components, i.e., turbulent kinetic energy profiles. The simple k-ε turbulence model with a fixed dissipation rate at the inlet [Eq. (3)] is unable to predict the principal features of a sudden expansion flowfield accurately. The calculations show reattachment at $X/H = 6$, as compared to the measured reattachment point of approximately 8 step heights. Furthermore, the calculations overpredicted the centerline velocity decay by up to 20%. The predictions of the radial mean velocity field were in error, especially at $X/H = 2$, which is not far from the prescribed initial condition. The agreement between the tangential mean velocity predictions and measurements were anticipated since the prescribed initial values were approximately zero. Figure 13d, which shows turbulent kinetic energy profiles, further highlights the differences between the experimental and numerical data. Accurate predictions of turbulent kinetic energy are important since turbulent transport phenomena must be considered when chemistry and spray submodels are incorporated in the solution scheme for performance evaluation of practical combustion systems.

For both swirl cases, Figs. 14 and 15, similar trends to those already described above were observed. However, the increased complexity of the swirling flowfields provided addi-

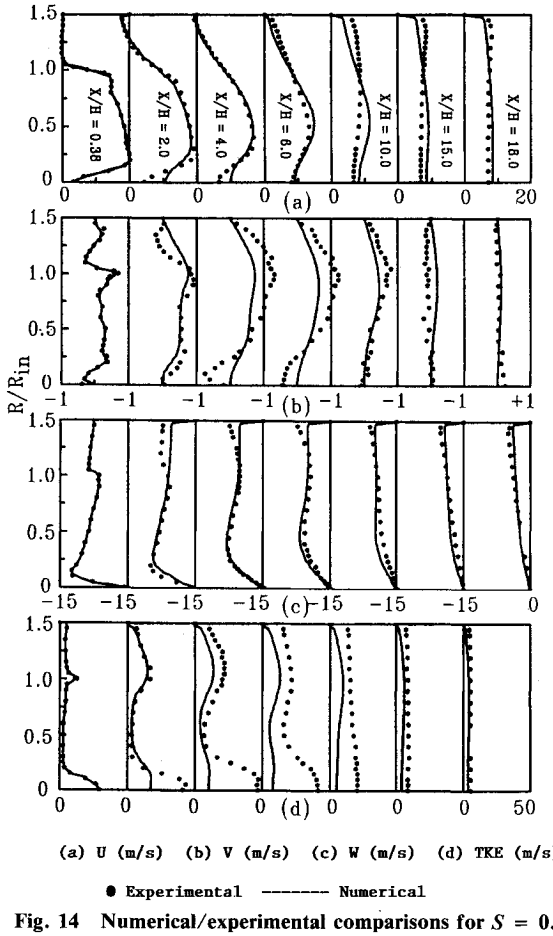

Fig. 14 Numerical/experimental comparisons for $S = 0.3$.

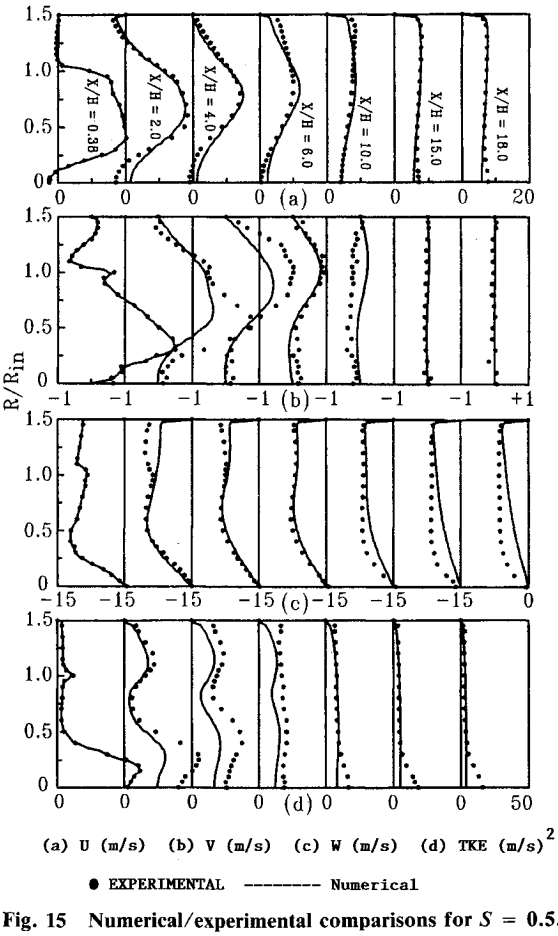

Fig. 15 Numerical/experimental comparisons for $S = 0.5$.

tional shear layers and recirculation regions which the numerical scheme failed to represent. For example, for $S = 0.5$, the calculations underpredicted the size and strength of the central recirculation region while simultaneously predicting the corner region adequately. Similar features were apparent for the $S = 0.3$ flow. Except in the far field ($X/H > 15$), the radial mean velocities were not predicted with any degree of accuracy, while the tangential components were depicted reasonably well, especially for $S = 0.3$.

As expected, large discrepancies between the numerical solution and the measurements of turbulent kinetic energy were observed in the swirling flows. These differences were most apparent in the $S = 0.3$ flow, which is known to be more unstable.[2,3] Large-scale oscillations contribute to the production of turbulent kinetic energy, and it is clear that steady-state calculations, such as the one employed in the current study, are unable to represent the effects of these oscillations.

The predicted strengths of the central and corner recirculation zones have been observed to be sensitive to the specification of the inlet length scale in Eq. (4). It is conceivable that a better agreement between the measurements and predictions could be achieved, for each individual flow, if this length scale is known with more certainty. The value (0.3) in the current study was chosen as the best compromise for simultaneous simulation of the three flows.

Conclusions

Swirl has a significant effect on the development of the combustor flowfield. The degree of swirl imparted to the flow can result in a central recirculation region (vortex breakdown), which can be of benefit to combustor performance by providing an additional flameholding zone. Further benefits include better mixing and the ability to decrease the overall length of the combustor without performance degradation.

A unique experimental setup was used to obtain detailed velocity measurements in an axisymmetric dump combustor with and without swirling inlet flow. Velocity and turbulence measurements were accomplished with a two-component LDV system. Measurements along the horizontal and the vertical diameters were taken to provide a near complete set of velocity data. Comparisons of the axial velocity components from each traverse (vertical, horizontal) at each measurement station proved the axisymmetry of the flowfield. Mass flow rate, based on integration of the axial velocity measurements, was conserved at each measurement station with the worst case error of 5%. In conclusion, it is believed that the current investigation is realistic in terms of the choices made in regard to swirl number values (sub/supercritical), swirl vane design, combustor geometry, and experimental techniques and provides a benchmark data base for CFD code validation.

Futhermore, a numerical solution algorithm, which utilized the k-ε closure model, was implemented in the current study. It was found that this scheme was not very successful in predicting the principal features of the flowfield investigated, even though a complete and accurate set of initial and boundary conditions were supplied for each case study. Further studies which aim to address the effects of chemical reaction and heat release in similar flowfields, both numerically and experimentally, are in progress.

Acknowledgments

This work was supported by the Air Force Office of Scientific Research with Julian Tishkoff as Technical Monitor.

References

[1]Buckley, P. L., Craig, R. R., and Schwartzkopf, K. G., "The Design and Combustion Performance of Practical Swirlers for Integral Rocket/Ramjets," *AIAA Journal*, Vol. 21, No. 5, 1983, pp. 733-740.

[2]Nejad, A. S., Favaloro, S. C., Vanka, S. P., Samimy, M., and Langenfeld, C., "Application of Laser Velocimetry for Characterization of Confined Swirling Flow," *Journal of Engineering for Gas Turbines and Power*, Vol. III, No. 1, 1989, pp. 36-45.

[3]Samimy, M., Nejad, A. S., Langenfeld, C. A., and Favaloro, S. C., "Oscillatory Behavior of Swirling Flows in a Dump Combustor," AIAA Paper 88-0189, 1988.

[4]Lilley, D. G., "Swirling Flows in Typical Combustor Geometries," AIAA Paper 85-0184, 1985.

[5]Rhode, D. L., Lilley, D. G., and McLaughlin, D. K., "Mean Flowfields in Axisymmetric Combustor Geometries with Swirl," *AIAA Journal*, Vol. 21, No. 4, 1983, pp. 593-600.

[6]Janjua, S. I., and McLaughlin, D. K., "Turbulence Measurements in a Swirling Confined Jet Flowfield Using a Triple Hot-wire Probe," Dynamics Technology, Torrance, CA, Rept. DT-8178-02, 1982.

[7]Fujii, S., Eguchi, K., and Gomi, M., "Swirling Jets With and Without Combustion," *AIAA Journal*, Vol. 19, No. 11, 1981, pp. 1438-1442.

[8]Sislian, J. P., and Cusworth, R. A., "Measurement of Mean Velocity and Turbulent Intensities in a Free Isothermal Jet," *AIAA Journal*, Vol. 24, No. 2, 1986, pp. 303-309.

[9]Gouldin, F. C., Depsky, J. S., and Lee, S-L., "Velocity Field Characteristics of a Swirling Flow Combustor," *AIAA Journal*, Vol. 23, No. 1, 1985, pp. 95-102.

[10]Vu, B. T., and Gouldin, F. C., "Flow Measurements in a Model Swirl Combustor," *AIAA Journal*, Vol. 20, No. 5, pp. 642-651.

[11]Habib, M. A., and Whitlaw, J. H., "Velocity Characteristics of Confined Coaxial Jets With and Without Swirl," *Journal of Fluids Engineering*, Vol. 102, No. 1, 1980, pp. 47-53.

[12]Ramos, J. I., and Somer, H. T., "Swirling Flow in a Research Combustor," *AIAA Journal*, Vol. 23, No. 2, 1985, pp. 241-248.

[13]Mattingly, J., and Oates, G., "An Experimental Investigation Of the Mixing of Co-annular Swirling Flows," *AIAA Journal*, Vol. 24, No. 5, 1986, pp. 785-792.

[14]Kuwatta, M., and Essenhigh, R. H., "Correlation of Pollutant Emissions, Noise and Heat Transfer in a Natural Gas Combustor," AIAA Paper 75-1267, 1975.

[15]Kilik, E., "Better Swirl Generation by Using Curved Vane Swirlers," AIAA Paper 85-1087, 1985.

[16]Beer, J. M., and Chigier, N. A., *Combustion Aerodynamics*, John Wiley and Sons, New York, 1972.

[17]Gupta, A. K., Lilley, D. G., and Syred, N., *Swirl Flows*, Abacus Press, Turnbridge Wells, England, 1984.

[18]Lilley, D. G., "Swirl Flows in Combustion: a Review," *AIAA Journal*, Vol. 15, No. 8, 1977, pp. 1063-1078.

[19]Craig, R. R., Nejad, A. S., Hahn, E. Y., and Schwartzkopf, K. G., "A General Approach for Obtaining Unbiased LDV Data in Highly Turbulent Non-Reacting and Reacting Flows," AIAA Paper 84-0366, 1984.

[20]Nejad, A. S., and Davis, D. L., "Velocity Bias in Two Component Individual Realization Laser Doppler Velocimetry," *Proceedings of the 5th International Congress on Application of Lasers and Electro Optics*, Laser Institute of America, Arlington, VA, Nov. 1986, pp. 78-89.

[21]McLaughlin, D. K., and Tiederman, W. G., "Biasing Correction for Individual Realization of Laser Anemometer Measurements in Turbulent Flows," *The Physics of Fluids*, Vol. 16, No. 12, 1973, pp. 2082-2088.

[22]Ahmed, S. A., Nejad, A. S., and Craig, R. R., "A Near Field Study of a Turbulent Free Jet, Including the Effects of Velocity Bias," *Eleventh Symposium on Turbulence*, Univ. of Missouri-Rolla, 1988.

[23]Snyder, P.K., Orloff, K. L. and Reinath, M. S., "Reduction of Flow Measurement Uncertainties in Laser Velocimeters with Nonorthogonal Channels," *AIAA Journal*, Vol. 22, No. 8, 1984, pp. 1115-1123.

[24]Vanka, S. P., "Block-Implicit Multigrid Solution of Navier-Stokes Equations in Primitive Variables," *Journal of Computational Physics*, Vol. 65, No. 1, 1986, pp. 138-147.

[25]Vanka, S. P., "Analytical Studies of Three-Dimensional Combustion Process," AFWAL-TR-88-2140, May 1989.

[26]Launder, B. E., and Spalding, D. B., "The Numerical Computation of Turbulent Flows," *Computer Methods in Applied Mechanics and Engineering*, Vol. 3, No. 2, 1974, pp 269-289.

[27]Hall, M. G., "Vortex Breakdown," *Annual Reviews of Fluid Mechanics*, Vol. 4, 1972, pp. 195-218.

[28]Liebovich, S., "Vortex Breakdown," *Annual Reviews of Fluid Mechanics*, Vol. 4, 1978, pp. 221-246.

[29]Liebovich, S., "Vortex Stability and Breakdown: Survey and Extension," *AIAA Journal*, Vol. 22, No. 9, 1984, pp. 1192-1206.